ANNUAL REPORT FOR NASA GRANT NAG 5-1239

GRANT
IN-89-CR
8138
P.31

by

Nebojsa Duric

University of New Mexico

The purpose of this report is to summarize the progress made under this proposal since August, 1990. The scientific goal of this proposal was to identify the emission components of spiral galaxies between 12 μm and 90 *cm* and to understand the relationships between them. The specific goal was to gain some understanding on the nature of the radio-infrared correlation. To this end we summarize the results below and we also list the new proposals that have been granted or are pending and which have directly resulted from this NASA grant.

List of Observing Proposals Granted

The following proposals have been granted on the basis of the results achieved under this proposal.

VLA: We have been granted 6 hours to observe our UV sample of galaxies at 3.8 *cm*. Combined with existing maps at lower frequencies these are being used to identify star forming regions within galaxies by separating the synchrotron and bremsstrahlung emission components on a pixel by pixel basis (next section). Our goal is to combine these with high resolution IRAS maps to study the IR-Radio correlation within individual galaxies.

NRAO - 12 meter *mm* telescope: We have been granted 36 hours to obtain integrated fluxes at 3*mm* for a fraction of our sample. This is invaluable to our effort to extract the integrated thermal bremsstrahlung component since it should dominate all other emission components at millimeter wavelengths.

IPAC: We have obtained add-scans for 140 galaxies and 2-D maps for all the galaxies in our sample that have diameters in excess of 1.5′. These have been analyzed in great detail and compared with the UV and radio data. The results of those comparisons are summarized below.

JAMES CLERK MAXWELL TELESCOPE: We have obtained 32 hours of telescope time to observe a sample of spiral galaxies at 400, 800, 1100 and 1300 microns. We have detected NGC 3079, NGC 4736 and NGC 5005 at 800 microns. Furthermore, we detected

NGC 3079 at 400 and 1100 microns and made maps of its nuclear region at 800 and 1100 microns.

Results

We have acted upon the work plan outlined in the last proposal and have come up with new results on the nature of the radio-infrared correlation in galaxies. The results are based on a refinement of the technique used to separate synchrotron and thermal bremsstrahlung radiation in spiral galaxies. The reprints and preprints outlining these results are enclosed. The list below summarizes the publications.

Publications Under This Proposal

Duric N., Price, R and Campbell, B. 1990: *B.A.A.S.*, **176**, 864

Dixon, D.S., Duric, N. and Slane, F. 1990: *B.A.A.S.*, **176**, 865

Duric, N. and Price, R. 1991: *Proc. 22nd Int Cosmic Ray Conf*, **2**, 169.

Duric, N. and Dixon, D. 1991: *Proc 22nd Int Cosmic Ray Conf*, **2**, 767.

Price, R. and Duric, N. 1992: Preprint (enclosed)

Talks Given

Multiwavelength Study of Nearby Spiral Galaxies, Price, R. - June 13, 1990: Albuquerque, NM

Resolution of Thermal and Synchrotron Emission Regions in NGC 3504, Dixon, D. - June 13, 1990: Albuquerque, NM

The Radio and Infrared Properties of Spiral Galaxies, Price, R. - June, 1991, Seattle, WA.

The Radio-Infrared Correlation of Galaxies, Duric, N. - August 24, 1991: Dublin, Ireland.

The Separation of Thermal and Synchrotron Radiation in Spiral Galaxies, Duric, N. - August 27, 1991: Dublin, Ireland.

New Results on the Radio-FIR Relation for Galaxies

Rob Price[1] *and Nebojsa Duric*

Institute for Astrophysics, University of New Mexico

[1]Infrared Processing and Analysis Center, California Institute of Technology

January 2, 1991 Draft

Abstract

We present new results that have a direct bearing on the interpretation of the radio-Far Infrared (FIR) relation for galaxies. By separating the thermal bremsstrahlung and synchrotron components of radio emission we have decomposed the radio-FIR relation into thermal bremsstrahlung-FIR and synchrotron-FIR relations for a sample of 31 galaxies. The new relations manifest strong correlations of their own. The thermal bremsstrahlung-FIR relation has a slope close to unity in log-log space (0.97 ± 0.02) while the synchrotron-FIR relation has a slope of 1.33 ± 0.10, significantly steeper than unity. These results shine new light on the radio-FIR relation and explain a number of previously unresolved issues.

• We find that both of the radio emission components are tightly correlated with the FIR emission for early and late-type spiral as well as irregular galaxies. It follows that any mixture of the radio components produces a tight universal radio-FIR relation.

• At high radio frequencies, thermal bremsstrahlung can dominate the radio emission over a larger range of luminosities so that the slope of the radio-FIR relation approaches that of the thermal bremsstrahlung-FIR relation and is therefore close to unity. At lower frequencies, synchrotron emission dominates and the slope approaches that of the synchrotron-FIR relation which is significantly steeper than unity. This result is consistent with the dependence of the radio-FIR slope on radio frequency found in the literature.

• Our results are consistent with a scenario in which the FIR luminosities of galaxies scale in direct proportion to the star formation rate (SFR) as determined from the thermal bremsstrahlung luminosity. However, the synchrotron luminosities scale as $\approx(\mathrm{SFR})^{1.2}$,

and not linearly as some previous reports have suggested.

I. Introduction

The now famous relationship between radio and far infrared (FIR) luminosities of galaxies has been the object of great scrutiny and debate over the past 5 years. The relation is universal among FIR and radio emitting galaxies where it holds over five orders of magnitude with a scatter of only ≈50% (see recent review by Helou 1990). When first reported as a linear relationship it was interpreted as representing a direct and linear relationship between star formation, FIR emission and the production of cosmic rays (de Jong *etal.* 1985; Helou *etal.* 1985). However, a number of issues have arisen that complicate this straightforward explanation. Recent studies have found that the slope of the $\log P_r$-$\log L_{fir}$ is not unity (see Table 1 for examples) and is in fact steeper than unity. The slopes of studies compiled in Table 1 in fact suggest a frequency dependence of the shape of the relation in the sense that, studies performed at frequencies lower than ≈5 GHz show the relation to be non-linear (ie. the log-log slope is generally greater than unity see Table 1), while above 5 GHz the slope of the relation is generally consistent with unity. It has been found by Wielebinski *et al.* (1987) and Wunderlich and Klein (1988) that at 5 GHz the slope of the $\log P_r$(P_r= radio power)-$\log L_{fir}$(L_{fir}=FIR luminosity) relation steepened from unity below $L_{fir} \approx 3.5 \times 10^{36}$ to ≈1.3 at higher luminosities. Chi and Wolfendale (1990) present evidence for a decreasing slope in the $\log P_r$-$\log L_{fir}$ relation with increasing L_{fir} at 1.49 GHz, but for a small range of galaxy luminosities and Hubble types.

The main complication in using the radio-FIR correlation to establish a direct link

between star formation and cosmic rays is the fact that the FIR emission consists of at least two emission components; cool (cirrus) dust and hot dust (Boulanger and Perault 1988). This makes the FIR-star formation linkage less obvious, since the cool dust emission may not be directly linked to the young stellar population. To obtain a more direct connection it is necessary to separate the hot FIR emission from the cool dust component to determine the amount of FIR emission that is being directly heated by the young stars. This has been a primary approach in trying to understand the radio-FIR correlation (Devereux and Eales 1989, Fitt *et al.* 1989). At present it is difficult to decouple the dust components because the physical properties and emission characteristics of the dust are poorly defined and the integrated IRAS fluxes do not provide sufficient spectral resolution.

In this paper we have chosen instead to decompose the *radio* emission into its fundamental emission mechanisms: synchrotron and thermal bremsstrahlung. This is an easier task than separating the dust components because the two radio emission mechanisms that have distinct and well-defined spectral characteristics and can be decoupled with multi-frequency radio observations which, for many galaxies, are readily available in the literature. The separation is motivated by the fact that thermal bremsstrahlung emission is directly proportional to the ionizing luminosity of stars on the upper end of the mass function and is therefore proportional to the SFR whereas synchrotron emission is directly proportional to the number density of relativistic electrons. The relationship between each of these components and the FIR then provides a path towards the establishment of a more direct physical link between the radio and the FIR emission com-

ponents. This approach also enables us to address the complications discussed above and thereby provides a sounder basis for understanding the nature of the radio-FIR relation.

The galaxy sample and the technique used for separating the synchrotron and thermal bremsstrahlung components are described in section II. Section III describes the results of the component radio-FIR relations and discusses the statistical tests which were performed to check the results. In section IV the consequences of these results on the interpretation of the radio-FIR correlation are discussed. A summary is presented in section V.

II. The Galaxy Sample and the Radio Separation Technique

a) Sample and Data

Our sample consists of those galaxies for which we could separate thermal bremsstrahlung and synchrotron components using integrated radio continuum spectra. To do this we started with ~120 spiral and irregular galaxies for which we found flux measurements at frequencies of $\gtrsim 10.7$ GHz (Israel and van der Hulst 1983, Gioia, Gregorini, and Klein 1982, Klein and Emerson 1981, Klein, Grave, and Wielebinski 1983, Klein, Weiland, and Brinks 1990, Wunderlich, Klein, and Wielebinski 1987). We then searched the literature using Nasa/IPAC Extragalactic Database (NED; Helou 1990) to find which of these galaxies (~100) had good spectral coverage of the radio continuum (ie. $\geq$4 observations between 408 MHz and 10.7 GHz). The final sample consists of the 31 galaxies for which we could reliably decompose the radio continuum into significant thermal bremsstrahlung

and synchrotron components (this technique is described below). We also discarded galaxies which are classified as Seyferts (to avoid the effects of active nuclei on integrated emission), but retain those classified as LINERS by Tully (1988). We emphasize that although these selection criteria bias the results (since our sample is composed of galaxies with large thermal bremsstrahlung emission components) it does allow us to isolate the effects of star formation on L_{fir}.

Monochromatic radio luminosities are used throughout this paper where the flux densities are taken from fits to the continuum data rather than the data itself. The 60 and 100 μm data are taken in order from (1) the large optical galaxy catalog (Rice *et al.* 1988), (2) the IRAS Bright Galaxy Sample (Soifer *et al.* 1989), (3) the IRAS small-scale structure catalog, and (4) the IRAS point-source catalog. FIR fluxes are calculated as prescribed in the IRAS Explanatory Supplements (1988). Distances, optical blue magnitudes and morphological types are from Tully (1988) and $H_o = 75$ km s^{-1} Mpc^{-1}.

b) Radio Separation Technique

Radio continuum spectra of spiral and irregular galaxies have been previously fit to examine the slope of the synchrotron spectrum and/or determine the amount of thermal bremsstrahlung emission (Condon 1983, Gioia and Gregorini 1984, Klein and Emerson 1981, Duric, Bourneuf, and Gregory 1988; hereafter DBG), In general these studies did not produce well-defined thermal bremsstrahlung components. The usual technique used for determining the thermal bremsstrahlung component is to fit a synchrotron spec-

trum to the low frequency flux densities and then place an upper limit on the thermal bremsstrahlung component at ~2 cm. The separation process used in this paper relies on the very different characteristics of the thermal and synchrotron continuum spectra at radio frequencies and follows the method of DBG. The two components are assumed to be optically thin, which on global scales is true for most galaxies (DBG), so the observed spectrum of a spiral galaxy is the result of a superposition of the two component spectra and a weighted least-squares fit of the equation

$$S_\nu = S_{syn}\nu^{-\alpha} + S_t\nu^{-0.1}$$

to the observed radio continuum spectrum is performed on each galaxy in our sample. S_{syn} represents the synchrotron component, α the spectral index, and S_t the thermal bremsstrahlung component of the radio emission. We have used the Levenburg-Marquardt routine for fitting non-linear curves presented in Press *et al* 1986 which searches for the minimum of the χ^2 space and computes errors of the component fluxes using the curvature matrix of the χ^2 space near the minimum. Our sample consists of those galaxies which had $\chi^2 \lesssim 3$ and thermal flux densities larger than their uncertainties. In a few cases (< 5) largely discrepant data points have been eliminated from the data.

III. The Radio-FIR Correlations

In this section we present the main results for the 31 galaxies for which we found significant thermal components as well as some tests that were performed to check these results. Figure 1 shows the radio-FIR relations at 5 GHz for a) the total radio, b) synchrotron, and c) thermal bremsstrahlung emission. Figure 1 d) plots the extracted

synchrotron component against the thermal bremsstrahlung component. Each figure contains a solid line representing the least squares fit to the data as well as the slope and correlation coefficient of the fit. The component relations (1b and c) have been fit using inverse error weighting and so the best fit lines lie near the upper envelope of the points where the errors are smaller. Figure 1a includes the best fit lines from the component relations (1b and c) to demonstrate the different dependences of the thermal bremsstrahlung and synchrotron components on the FIR emission. The steep slope of the synchrotron-FIR relation (1.33 ± 0.10) shows that the synchrotron emission component dominates the radio emission at higher luminosities, while the thermal bremsstrahlung-FIR relation has a slope of 0.97 ± 0.02 which dominates the radio emission at lower luminosities. The correlation coefficients of the component relations (0.91 for synchrotron-FIR and 0.92 for thermal-FIR) verify the surprisingly tight correlations seen in Figs. 1b and c. We discuss the likelihood of these tight correlations being produced by a random extraction process at the end of this section. Figure 1d shows the non-linear dependence of the synchrotron emission on the thermal bremsstrahlung component (slope=1.22 ± 0.18) which has a reasonable correlation coefficient of 0.78 considering the large uncertainty of the extraction process that is inherent in each component.

In each of the plots in Fig 1 the galaxies have been divided by their morphological types into early (Sa to Sbc), late (Sc to Sdm), and irregular (including 6 blue compact dwarf galaxies). The morphological class distributions are indistinguishable from one another on these plots which implies that the total radio, thermal bremsstrahlung, synchrotron and FIR emission from galaxies have a similar interdependence regardless of

galaxy type.

Figure 2 presents a complementary view of the results in Fig 1. Radio-FIR correlations have been constructed for our sample of 31 galaxies at four different wavelengths using flux densities that have been obtained from the best fit curves to the radio continuum data. This was done in order to illustrate the effect of the relation in Figs. 1b and 1c on the total radio-FIR correlation. The high frequency (2 cm) radio-FIR plot has a slope close to unity while those with decreasing frequencies exhibit steepening slopes approaching the slope of the synchrotron-FIR relation of Fig 1b. This is consistent with our Fig 1 results since the high frequency (2 cm) emission is thermal bremsstrahlung dominated and should therefore have a slope close the that of unity as in our extracted thermal bremsstrahlung-FIR relation of Fig 1c. As the frequency decreases the synchrotron fraction of the radio emission increases (owing to the steeper spectrum of synchrotron emission) and the slope of the radio-FIR relation tends toward the steeper value of the extracted synchrotron-FIR relation of Fig 1b. It is interesting to note that the 20 cm and 75 cm plots are still not as steep as the synchrotron-FIR relation since some of the galaxies in our sample still have a noticeable amount of thermal bremsstrahlung emission even at these long wavelengths. This is because our sample is biased toward galaxies with larger thermal fractions. The increasing slope of the radio-FIR relation with wavelength provides confirmation of our two basic results that the synchrotron component has a non-linear dependence on FIR while the thermal bremsstrahlung component has a linear dependence.

We investigated whether these relations are caused by mass effects (where more massive galaxies produce more energy in any measurable spectral regime) by normalizing the plotted parameters with blue luminosities and linear area (kpc^2). The correlation coefficients of the Fig 1 relations normalized by blue luminosity were reduced to 0.93, 0.84, 0.77, and 0.53, respectively, and to 0.96, 0.89, 0.87, and 0.71 when the relations were normalized by linear area. This indicates that correlations of Fig 1 are still significant after normalization and therefore not merely a product of the mass effect.

Lastly, we examine the possibility that the component-FIR relations have been produced by a random process. This was done in anticipation that the initially very tight correlation could produce very tight component correlations even if a random process was invoked to extract the components. To check this we made a 1000 runs of a program that took random fractions of the total radio flux of each point in Fig 1a and then formed 1000 random thermal-FIR and random synchrotron-FIR relations. Least squares fits of the random relations gave distributions of 1000 correlation coefficients and slopes for comparison with those of our data. We found that simultaneous correlation coefficients of larger than 0.92 for random thermal-FIR and 0.91 for the random synchrotron-FIR relations occurred $<0.5\%$ of the time. In fact simultaneous correlation coefficients of greater than 0.9 occur only 1.3% of the time. Random single component correlation coefficients of >0.92 occur $\approx 6\%$ of the time and slopes as large as 1.33 only 0.7% of the time. These results indicate that our component relations in Figs 1b and c have a very small probability of being generated by a purely random separation process. We suggest instead that the reduction in the correlation coefficient in going from Fig 1a to Figs 1b and 1c is

produced largely by the uncertainties introduced by the radio separation techniques.

IV. Discussion

The above results show that the radio components are both tightly correlated with the FIR emission, but with different dependences. We suggest here that the different slopes of the synchrotron-FIR and thermal bremsstrahlung-FIR relations can account for the universality of the radio-FIR correlation as well as a number of its peculiarities. These results also provide strong constraints for understanding the radio-FIR relation by directly linking the FIR emission with the individual radio emission components.

a) Universality

The strong correlations between each of the radio components and the FIR explain why such a wide variety of galaxies obey the same *universal* radio-FIR correlation. The galaxy types that adhere to the same radio-FIR relation range from starburst and BCD galaxies through late and early type spirals to S0 and elliptical galaxies (Helou 1990). Because these galaxy types span a wide range of star formation rates, dust properties, and magnetic field strengths one would expect them to have drastically different mixtures of synchrotron, thermal bremsstrahlung, and FIR emission and therefore not expect them to obey the same radio-FIR relation. However, over the range of morphological types, Sa to BCDGs (blue compact dwarf galaxies), displayed in Figs 1b and c, there is no apparent dependence of these component relations on morphological type. The synchrotron and thermal bremsstrahlung components have the same dependence on L_{fir}

independent of galaxy type and therefore, regardless of the mixture of synchrotron and thermal bremsstrahlung emission within a galaxy, the total radio emission will obey the global radio-FIR correlation. These component relationships therefore provide key information in understanding the universal radio-FIR correlation and bring us closer to the underlying physical mechanisms that generate the radio and FIR emission in galaxies.

b) L_{fir} Dependence

Recent studies of large samples of galaxies have found that the radio-FIR correlation is non-linear as shown by the non-unity of the slope in log-log space (Devereux and Eales 1989, Condon *et al.* 1991). Our Figs 1 and 2 confirm these results and the claim of these and other authors that the synchrotron component of the radio emission is responsible for the non-linearity of the radio-FIR correlation. We also show that the thermal bremsstrahlung and FIR emission are linearly related. As a result of the different dependences of these components on the FIR emission the ratio of thermal to synchrotron emission is a function of L_{fir}. This can be seen in Fig 1a where the best fit synchrotron and thermal bremsstrahlung curves cross at $\log L_{fir} \sim 37.0$, which is consistent with the slope crossover found by Wunderlich and Klein (1988). The thermal fraction of the radio emission therefore decreases with increasing L_{fir}.

A second consequence of the differing slopes is that at wavelengths where the thermal bremsstrahlung and synchrotron contributions are roughly equal there will be a steepening in the slope of the radio-FIR relation with increasing L_{fir}. Such a curvature in

the radio-FIR relation has been observed at 4.75 GHz by Wielebinski *et al.* (1987) and Wunderlich and Klein (1988) who found a slope of 0.99±0.38 below $\log L_{fir} \approx 36.54$ and 1.26±0.33 at higher L_{fir}. In checking the relations in Fig 2 for a change in slope above and below $L_{fir} \sim 36.5$ we found, at 2 and 6 cm, that the slope steepened with L_{fir}, while at 20 cm the slope remained the same and at 75 cm it was steeper at lower L_{fir}. Note that for all these results, however, including those of Wunderlich and Klein (1988), the slopes are consistent, within the errors, with unity. Our low frequency results follow those reported at 20 cm by Chi and Wolfendale (1990) who found that their radio-FIR relation flattened with increasing L_{fir}. They also developed a cosmic-ray escape model that predicted such a trend for pure synchrotron-FIR relations. We further note that the slope of our synchrotron-FIR relation flattened with increasing L_{fir} while our thermal bremsstrahlung-FIR relation steepened above L_{fir}, but refrain from over-interpreting these highly uncertain results.

c) Radio Frequency Dependence

As seen in Fig 2 and discussed in section III the slope of the radio-FIR relation changes with frequency of the radio observations. At high frequencies the thermal bremsstrahlung component dominates the radio emission (owing to its flatter spectrum) so that the radio-FIR relation in Fig 2 at 2 cm approximates the thermal bremsstrahlung-FIR case in Fig 1c where both relations are close to being linear. At lower frequencies, the synchrotron emission dominates the radio emission and hence the radio-FIR relation in Fig 2 at 75 cm approaches the synchrotron-FIR case in Fig 1b. This effect is also

apparent in previously published results. In Table 1 we have compiled results from the literature to study the dependence of the radio-FIR slope on the frequency of the radio observations. The high frequency ($\geq$5 GHz) studies have slopes consistent with unity (0.9–1.0), while at lower frequencies the slopes are generally greater than unity (1.1–1.3). The radio frequency dependence of the slope found in published results is then consistent with the results presented in this paper.

d) The Role of Star Formation

Our above results have been presented to display their consistency with each other and previously reported results on the radio-FIR correlation. In this letter we briefly mention some of the implications of our results that link the underlying physical mechanisms of the relation. Previous authors had in general surmised that the non-linear nature of the radio-FIR relation involved the synchrotron component of the radio emission (Fitt *et al.* 1988, Devereux and Eales 1989). However, attempts to linearize the radio-FIR relation were made by estimating the FIR contribution of the the cool dust component and then subtracting it out (Fitt *et al.* 1988, Devereux and Eales 1989). This produced a linear relation between the extracted hot dust component and the radio emission and it was concluded that both components were directly and linearly related to star formation. More recently Condon, Anderson, and Helou (1991) were unsuccessful in using their techniques to linearize the radio-FIR relation for two large galaxy samples.

We, on the other hand, have obtained a direct measure of the star formation rates of

our 31 galaxies through the thermal bremsstrahlung components. The thermal bremsstrahlung power, P_t, is a measure of the luminosity of ionizing photons which come from the upper end of the luminosity function. Since this is the region of the IMF where the population of ionizing stars can exist in equilibrium with the SFR, P_t then represents the SFR. Since P_t and L_{fir} are linearly related we conclude that L_{fir} must scale with the SFR. To reconcile this with a two temperature dust model for the FIR emission, where up to 70% of the Galactic FIR emission is in the form of cirrus (Boulanger and Perault, 1988), we conclude that either star formation heats both dust components or the population heating the cool dust scales linearly with the number of young stars (which produce the hot dust emission). It is beyond the scope of this paper to attempt to differentiate between these two possibilities. The non-linear dependence of synchrotron emission on both the thermal bremsstrahlung and FIR emission implies that the synchrotron emission is related to the star formation rate as $\approx(\mathrm{SFR})^{1.2}$. We do not find this to be a surprising result because, while the number of cosmic rays generated may be linearly related to star formation, the other properties that govern synchrotron radiation (such as magnetic field strength and cosmic ray electron lifetime) are not necessarily linearly related to star formation. The results we have presented may lead to a new scenario in which star formation accounts for both L_{fir} and P_{syn}, but not in the manner previously formulated. The physical interpretation of this relation and the details of the data selection will be discussed in a future paper.

V. Summary

Separating the radio continuum into thermal bremsstrahlung and synchrotron com-

ponents has led to potentially new insights into the nature of the radio-FIR correlation. The thermal bremsstrahlung emission is linearly related to the FIR emission, which implies a direct dependence of FIR on star formation. The synchrotron emission is non-linearly related to both FIR and SFR, with the power law dependence being larger than unity. These tight relations explain why the radio-FIR correlation encompasses itself in so many different types of galaxies, with large differences in the mix of thermal bremsstrahlung and synchrotron radio emission. We find that the slope of the radio-FIR correlation steepens with radio wavelength in a manner that is completely consistent with our component relations since it increases from unity at short wavelengths where the thermal bremsstrahlung dominates the radio emission to 1.15 at 75 cm where the synchrotron emission is dominant. The previously reported steepening of the radio-FIR relation with L_{fir} at 5 GHz is explained by the steeper synchrotron-FIR correlation dominating the thermal bremsstrahlung relation at larger L_{fir}.

Acknowledgements

We thank George Helou, David Clarke, and Shawn Gordon for helpful discussions. This work was supported by NASA grant NAG 5-1239. RP gratefully acknowledges a summer research assistantship from IPAC.

References

Boulanger, F. & Perault, M. 1988, ApJ, 330, 964

Chi, X & Wolfendale, A.W. 1990, MNRAS, 245, 101

Cox, M.J., Eales, S.A.E., Alexander, P., & Fitt, A.J. 1988, MNRAS, 235, 1227

Condon, J.J., Anderson, M.L., & Helou, G. 1991, preprint

de Jong, T., Klein, U., Wielebinski, R., & Wunderlich, E. 1985, A&A, 147, L6

Devereux, N.A. & Eales, S.A. 1989, ApJ, 340, 708

Duric, N. 1988, Ap&SS, 48, 73

Duric, N., Bourneuf, E., & Gregory, P.C. 1988, AJ, 96, 81 (DBG)

Fitt, A.J., Alexander, P., & Cox, M.J. 1988, MNRAS, 233, 907

Gavazzi, G., Cocito, A., & Vettolani, G. 1986, ApJL, 305, L15

Helou, G. 1990, in The Interpretation of Modern Synthesis Observations of Spiral Galaxies, edited by N. Duric and P. Crane, in Vol 18, Publication of the ASP

Helou, G., Soifer, B.T., & Rowan-Robinson, M. 1985, ApJL, 298, L7

Hummel, E., Davies, R.D., Wolstencroft, R.D., van der Hulst, J.M., & Pedlar, A. 1988, A&A, 199, 91

Klein, U., Weiland, H, & Brinks, E. 1991, A&A, in press

Press, W.H., Flannery, B.P., Teukolsky, S.A., & Vetterling, W.T. 1986 Numerical Recipes (Cambridge University Press, Cambridge), p523

Rengarajan, T.N. & Iyengar, K.V.K. 1990, MNRAS, 242, 74

Rice, W., *et al.* 1988, ApJS, 68, 91

Soifer, B.T., Boehmer, L., Neugebauer, G., & Sanders, D.B. 1989, AJ, 98, 766

Tully, R.B. 1988, Nearby Galaxies Catalog (Cambridge University Press, Cambridge)

Unger, S.W., Wolstencroft, R.D., Pedlar, A., Savage, A., Clowes, R.G. Leggett, S.K., & Parker, Q.A. 1989, 236, 425

Wielebinski, R., Wunderlich, E., Klein, U., & Hummel, E. 1987, in Star Formation in Galaxies, edited by C.J. Lonsdale Persson, NASA Conference Publication 2466, p 589

Wunderlich, E. & Klein, U. 1988, A&A, 206, 47

TABLE 1
Summary of Radio-FIR Correlations

Freq. (GHz)	No. of Galaxies	Slope	Corr Coeff	Ref.	Galaxy Sample
10.7	74	1.02±0.03	0.97	1	early IRAS detections
4.75	91	0.94±0.06[a]		2	"
4.75	99	0.99±0.38[b]		3	"
4.75	99	1.26±0.33[c]		3	"
4.75	74	0.98±0.03	0.97	1	"
2.3	198	1.20	0.91	4	S,S0,Irr
1.5	100	1.1±0.1[d]		5	Sbc
1.49	237	1.28±0.03		6	RSA spirals
1.49	62	1.17		7	"
1.49	250	1.29±0.02		8	"
1.49	258	1.11±0.02		8	IRAS BGS
1.4	38	1.1[a]		9	Virgo,field,starburst
1.4	12	1.25[a]		10	Hercules spirals
0.408	120	1.02±0.06	0.84	1	S,S0,Irr
0.151	65	1.16±0.04	0.96	11	6C radio

[1]Rengarajan and Iyengar (1990)
[2]de Jong *et al.* (1985)
[3]Wunderlich and Klein (1988)
[4]Gavazzi, Cocito, and Vettolani (1986)
[5]Hummel *et al.* (1988)
[6]Devereux and Eales (1989)
[7]Chi and Wolfendale (1990)
[8]Condon, Anderson, and Helou (1991)
[9]Helou, Soifer, and Rowan-Robinson (1985)
[10]Dickey and Salpeter (1984)
[11]Fitt, Alexander, and Cox (1988)

[a]flux-flux
[b]$L_{fir} < 3.5 \times 10^{36}$ W
[c]$L_{fir} > 3.5 \times 10^{36}$ W
[d]used $L_{100\mu m}$

Figure Captions

Fig. 1: For 31 galaxies for which we have extracted thermal and synchrotron radio components we plot at 5 GHz a) total radio-FIR, b) synchrotron-FIR, c) thermal bremsstrahlung-FIR, and d) synchrotron- thermal bremsstrahlung. In each case the solid line is the least squares fit with uniform weighting in a) and d) and inverse error weighting in b) and c). The slopes and correlation coefficients of the best fits are also listed on each plot. Figure 1 a also contains the best fits of Figs 1b and c to demonstrate the differences in their slopes and how their ratio varies with L_{fir}. The galaxy types are designated as early (Sa-Sbc), late (Sc-Sdm), and irregular (including 6 blue compact dwarf galaxies.

Fig. 2: For each of the 31 galaxies with thermal and synchrotron components we plot total radio-FIR relations at 2, 6, 20, and 75 cm. The radio fluxes are obtained from the best fit curves to the radio continuum data. Least square fits to the data are drawn on each plot along with their slopes and correlation coefficients. The plots clearly show that the slope of the radio-FIR correlation increases with wavelength.

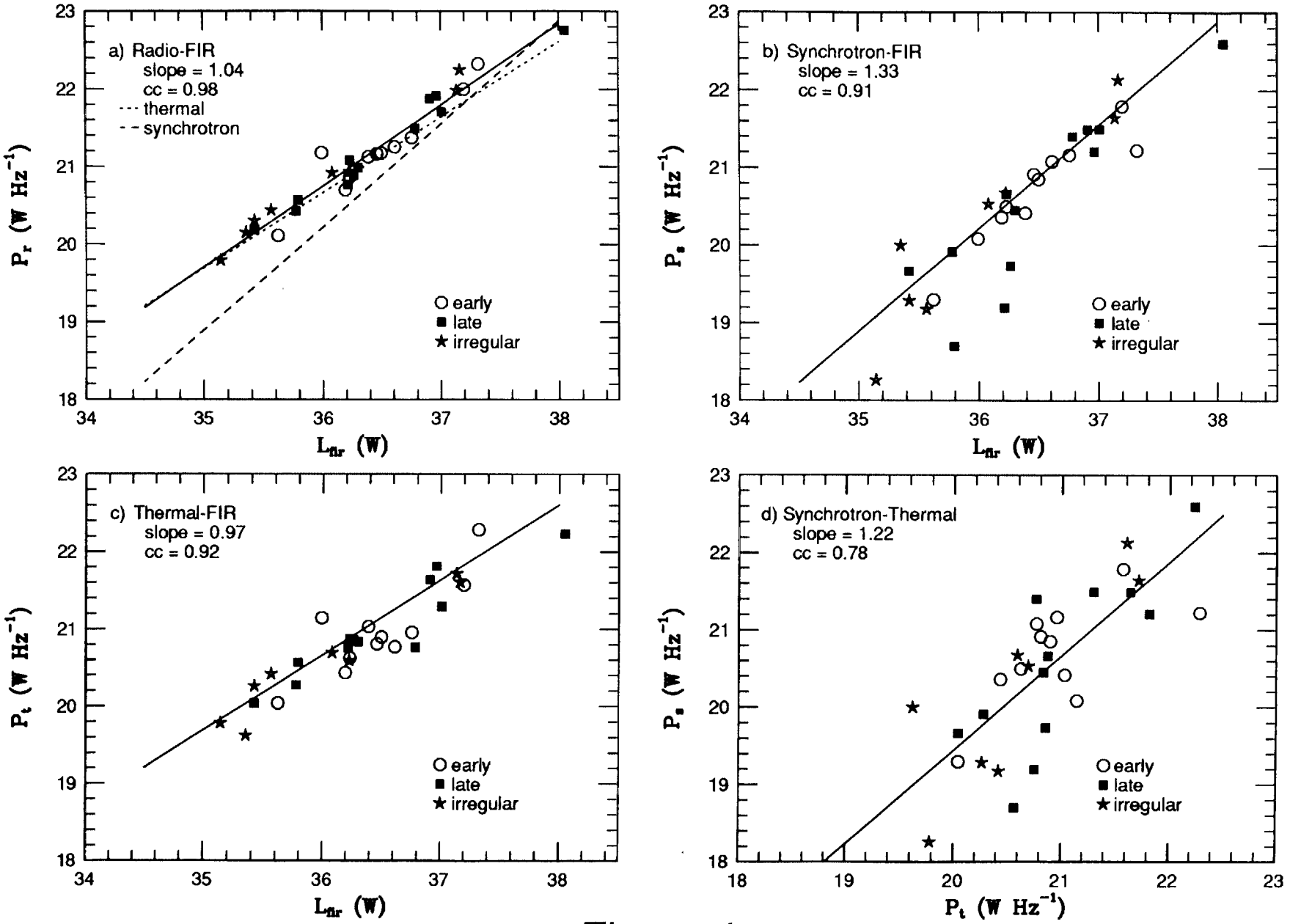
a) Radio-FIR
slope = 1.04
cc = 0.98
--- thermal
- - synchrotron
O early
■ late
★ irregular
P_r (W Hz^{-1})
L_{fir} (W)
b) Synchrotron-FIR
slope = 1.33
cc = 0.91
P_s (W Hz^{-1})
c) Thermal-FIR
slope = 0.97
cc = 0.92
P_t (W Hz^{-1})
d) Synchrotron-Thermal
slope = 1.22
cc = 0.78

Figure 1

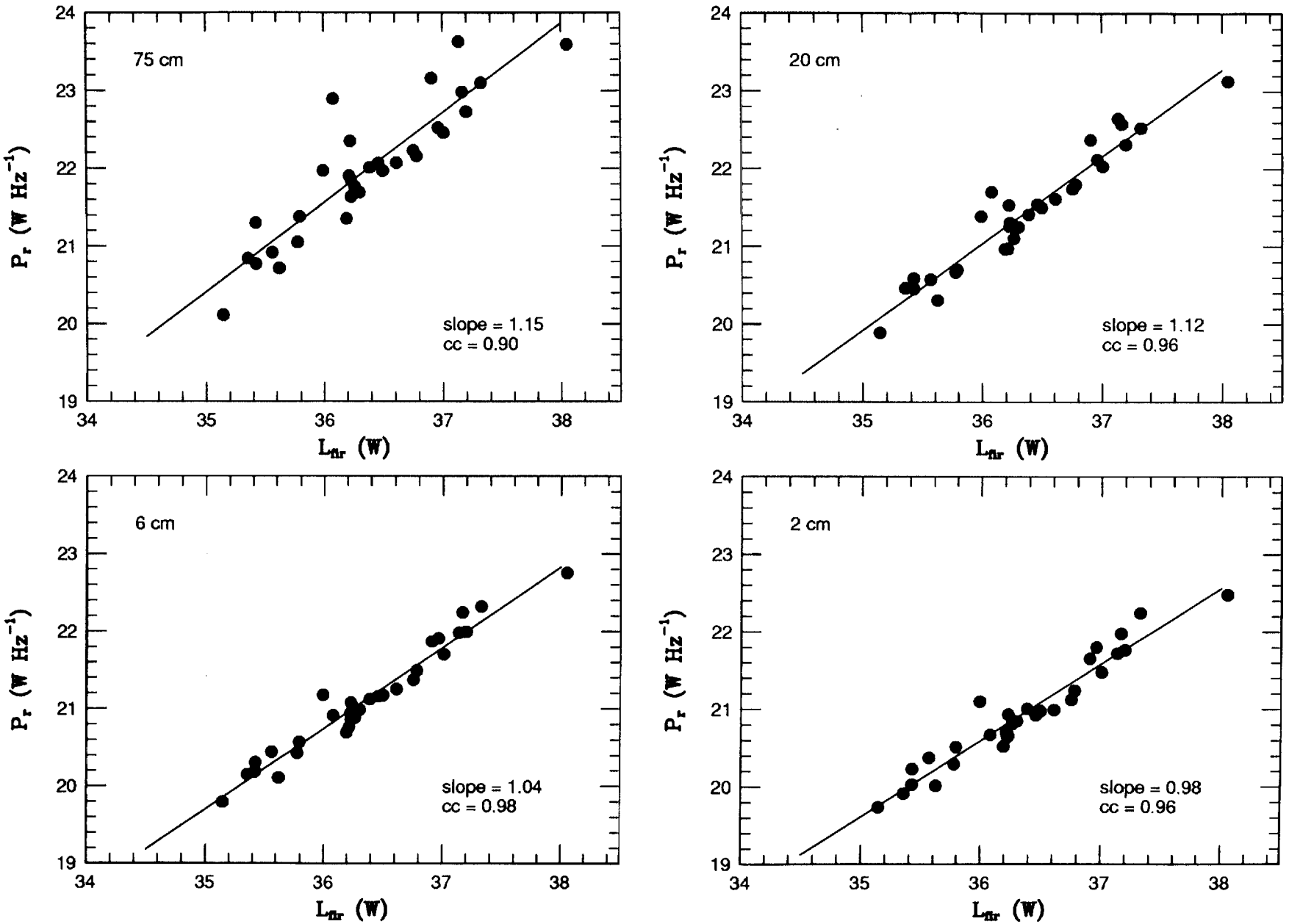
75 cm
slope = 1.15
cc = 0.90
20 cm
slope = 1.12
cc = 0.96
6 cm
slope = 1.04
cc = 0.98
2 cm
slope = 0.98
cc = 0.96
P_r (W Hz^{-1})
L_{fir} (W)
19
20
21
22
23
24
34
35
36
37
38

Figure 2

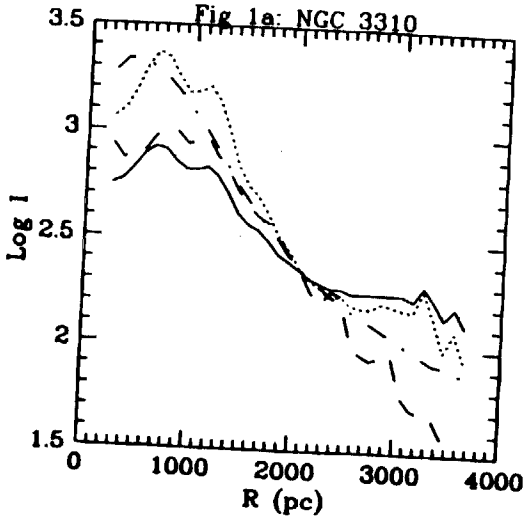

Fig 1a: Radial profiles of the light distribution in NGC 3310. The solid curve represents the CR electron distribution assuming equipartition. The dotted curve is that of the radio continuum emission at a wavelength of 20 cm. The Hα emission is shown as the dashed curve. It represents the distribution of ionized gas associated with regions of star formation. The light of the older, population II stars is shown as the dot-dash curve. The vertical scale is logarithmic and all curves are normalised at 2 kpc.

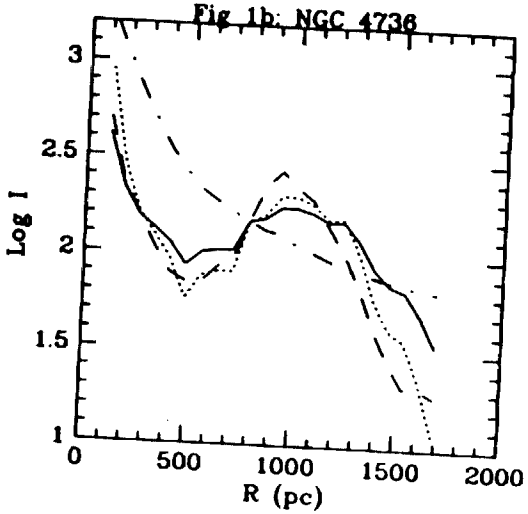

Fig 1b: Radial profiles of the light distribution in NGC 4736. The legend is as above. Curves are normalized at 0.8 kpc.

THE RADIO-INFRARED CORRELATION OF GALAXIES

Nebojsa Duric and Rob Price
Institute for Astrophysics
Department of Physics and Astronomy
University of New Mexico
Albuquerque, NM 87131
U.S.A.

Abstract

We present new results that have a direct bearing on the interpretation of the radio-FIR relation for galaxies. By separating the thermal bremsstrahlung and synchrotron components of radio emission we have decomposed the radio-FIR relation into thermal bremsstrahlung-FIR and synchrotron-FIR relations for a sample of spiral and dwarf galaxies. The thermal bremsstrahlung-FIR relation has a slope close to unity in log-log space (0.9 ± 0.1) but the synchrotron-FIR relation has a slope of 1.4 ± 0.1, significantly steeper than unity. These results explain a number of previously unresolved issues.

Introduction The main complication in establishing a direct linkage between star formation and cosmic ray production via the radio-FIR relation is the multi-component nature of the dust emission. To obtain a more direct connection one would like to separate the FIR emission from galaxies into its various dust components and then determine which are directly heated by young stars. At present this approach is very difficult since the physical properties and emission characteristics of the dust are poorly defined. In this paper we concentrate instead on decomposing the *radio* emission into its fundamental emission mechanisms: synchrotron and thermal bremsstrahlung. This is an easier task than separating the dust components since we are dealing with two distinct emission mechanisms that have well-defined continuum spectral characteristics. The dependence of the FIR on these components provides a path towards a more direct physical linkage between the radio and the FIR emission components which may ultimately provide new insight into the origin of cosmic rays (CR).

The technique used here is similar to that of Duric, Bourneuf, and Gregory (1988). The separation process is based on the very different characteristics of the thermal and synchrotron continuum spectra at radio frequencies. Assuming that the observed spectrum of a spiral galaxy is the result of a superposition of these two spectra we have performed a weighted least-squares fit of the equation

$$S_\nu = S_{syn}\nu^{-\alpha} + S_t\nu^{-0.1}$$

to the observed radio continuum spectrum of each galaxy in our sample. S_{syn} represents the synchrotron emission, α the spectral index, and S_t the thermal

bremsstrahlung component of the radio emission. We have used the Levenburg-Marquardt routines for fitting non-linear curves provided by Press *et al* 1986. The errors are computed using the curvature matrix of the χ^2 space near minimum.

Results Of the 46 galaxies in our sample, thermal components were extracted for 18 galaxies and 3σ upper limits were obtained for all other galaxies. In figures 1, 2, and 3 we present the radio-FIR relations for the total radio, synchrotron, and thermal bremsstrahlung emission respectively for the sample of galaxies with well-determined thermal components. The solid lines on each figure indicate uniformly weighted linear least squares fits. Figure 1 also includes the best fit lines from the component relations to demonstrate that the thermal bremsstrahlung and synchrotron components have significantly different dependence on the FIR emission. The steep slope of the synchrotron-FIR relation (1.4±0.1) shows that the synchrotron emission component dominates the radio emission at higher luminosity, while the thermal bremsstrahlung-FIR relation has a slope of 0.9±0.1 which dominates the radio emission at lower luminosities. The correlation coefficients of the component relations (0.93 and 0.94 respectively) confirm the surprisingly tight correlations evident in figures 2 and 3. We note that although the size of the sample is relatively small it covers roughly two orders of magnitude in luminosity. We are therefore confident that the effects here are real and that the synchrotron and thermal bremsstrahlung correlations have significantly different slopes.

We examined the possibility that the component-FIR relations might be the result of random processes. We generated 1000 runs of a program which applies random fractions, between 0.0 and 1.0, to the total radio flux of each point in Fig 1 and then formed 1000 random thermal-FIR and random synchrotron-FIR relations. Least squares fits of the random relations gave distributions of 1000 correlation coefficients and slopes for comparison with those of our data. We found that the probability of having correlation coefficients larger than 0.93 for random thermal-FIR and 0.94 for the random synchrotron-FIR relations was <0.01. In fact simultaneous correlation coefficients of greater than 0.9 occur only 1.3% of the time. Random single component correlation coefficients of >0.93 occur ≈5% of the time and slopes as large as 1.4 only 2% of the time. These results indicate that our component relations (figures 2 and 3) are not likely to have been generated by a purely random process.

Discussion We propose that the different slopes of the synchrotron-FIR and thermal bremsstrahlung-FIR relations may account for the universality of the radio-FIR correlation as well as a number of its peculiarities. These results also provide strong constraints for understanding the relation by directly linking the FIR emission with the individual radio emission components.

The strong correlations between each of the radio components and the FIR explain why such a wide variety of galaxies obey the same *universal* radio-FIR correlation. The galaxy types that adhere to the radio-FIR relation range from starburst and

blue compact dwarf (BCD) galaxies through late and early type spirals to S0 and elliptical galaxies. Because these galaxy types potentially span a wide range of star formation rates, dust properties, CR abundances and magnetic field strengths one would expect them to have drastically different mixtures of synchrotron, thermal bremsstrahlung, and FIR emission. Our sample of spiral and BCD galaxies shows that each of the radio components may be tightly correlated with the FIR emission. This implies that regardless of the mixture of synchrotron and thermal bremsstrahlung emission in a galaxy its total radio emission will still obey the radio-FIR correlation.

Recent studies of large samples of galaxies have found that the radio-FIR correlation is non-linear as shown by the non-unity of the slope in log-log space (Devereux and Eales 1989, Condon *et al.* 1991). In figures 2 and 3 we see that the synchrotron-FIR relation is non-linear, while the thermal bremsstrahlung-FIR relation is close to linear. These results enable us to predict the dependence of the slope of the radio-FIR relation on the FIR luminosity and radio frequency. The faint end of the relation is closer to the flatter thermal bremsstrahlung-FIR case while the bright end resembles the steeper synchrotron-FIR case which leads to a curvature in the sense that has been observed at 4.75 GHz by Wielebinski *et al.* (1987) and Wunderlich and Klein (1988).

The slope of the radio-FIR relation will also change with radio frequency. At high frequencies the thermal bremsstrahlung component dominates the radio emission (owing to its flatter spectrum) so that the radio-FIR relation approximates the thermal bremsstrahlung-FIR case which is close to being a linear relation. At lower frequencies, the synchrotron emission dominates the radio emission and hence the radio-FIR approaches the synchrotron-FIR case. We have compiled results from the literature to study the dependence of the radio-FIR slope on the frequency of the radio observations. The high frequency (≥5 GHz) studies have slopes consistent with unity (0.9–1.0), while at lower frequencies the slopes are generally greater than unity (1.1–1.3). The radio frequency dependence of the slope appears to be consistent with our predictions.

Perhaps the most interesting consequence of our results lies in the relationship between the radio components and the FIR emission. The dependence of P_t on L_{fir} suggests that there is a linear relation between L_{fir} and the star formation rate. To reconcile this with a two temperature dust model for the FIR emission, where up to 70% of the Galactic FIR emission is in the form of cirrus, we must conclude that either star formation heats both dust components or the population heating the cool dust scales with the number of young stars (which produce the hot dust emission). It is beyond the scope of this paper to attempt to differentiate between these two possibilities. Based on the linear dependence of thermal bremsstrahlung on the SFR, we find that the synchrotron luminosity $\propto(\mathrm{SFR})^{\alpha}$ where $\alpha \approx 1.3$. This result, coupled with the linearity between the L_{fir} and P_t leads to a new scenario in which star formation *can* account for both the L_{fir} and P_{syn} thereby establishing once again the notion that star formation and CR production are linked.

References
Condon, J.J., Anderson, M.L., and Helou, G. 1991, preprint
Devereux, N.A. and Eales, S.A. 1989, ApJ, 340, 708
Duric, N., Bourneuf, E., and Gregory, P.C. 1988, AJ, 96, 81
Klein, U., Weiland, H., and Brinks, E. 1991, *Astr.Ap.,In Press*
Press, W.H., Flannery, B.P., Teukolsky, S.A., and Vetterling, W.T. 1986 Numerical Recipes (Cambridge University Press, Cambridge), p523
Soifer, B.T. et al. 1989, *A. J.*,98, 766
Wielebinski, R., Wunderlich, E., Klein, U., and Hummel, E. 1987, in Star Formation in Galaxies, edited by C.J. Lonsdale Persson, NASA Conference Publication 2466, p 589
Wunderlich, E. and Klein, U. 1988, A&A, 206, 47

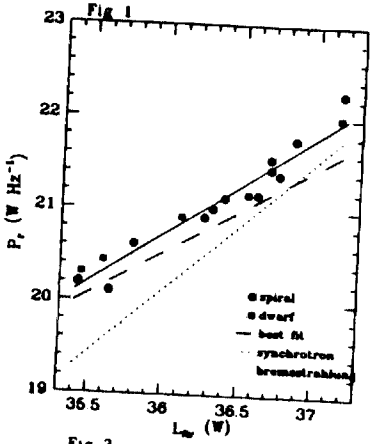

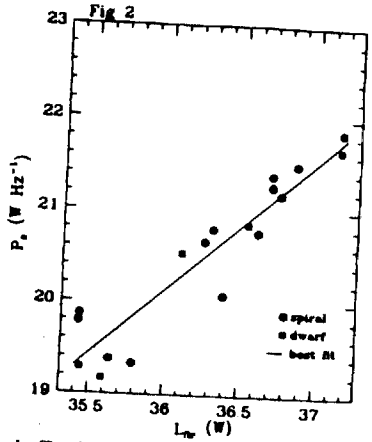

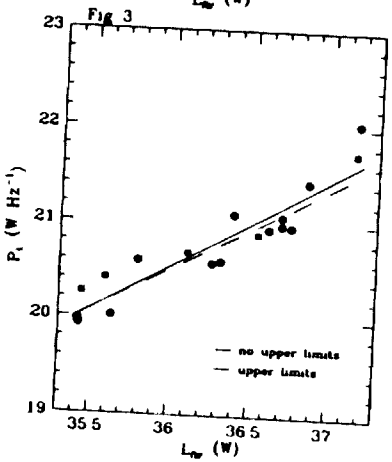

Fig 1: Total radio power at 5 GHz is plotted against L_{fir} for 13 spiral galaxies and 5 BCD galaxies. For the spiral galaxies the radio data is from Duric *et al.* (1988) and the FIR data is from Soifer *et al.* (1988). The BCD galaxy data is from Klein *et al.* (1990). The curves represent the best fit to the total radio data (solid), synchrotron radio (long dashed), and thermal bremsstrahlung radio (short dashed) vs. L_{fir}.
Fig 2: Extracted synchrotron power at 5 GHz plotted against L_{fir}. The slope of the relation is significantly different from unity.
Fig 3: Extracted thermal bremsstrahlung power at 5 GHz plotted against L_{fir}. The solid line is a uniformly weighted least squares fit to the circled points and the dashed line is a least squares fit that includes the upper limit using survival analysis techniques.

SEARCH FOR PRIMORDIAL ANTIMATTER WITH ANTARCTIC BALLOON FLIGHTS

M.Aglietta[1], C.Castagnoli[1], A.Castellina[1], R.Fujii[2], Y.Fukada[3], W.Fulgione[1], P.Galeotti[1], Y.Hatano[3], T.Hara[3], M.Kusunose[4], H.Oda[5], O.Saavedra[1], T.Saito[3], G.Trinchero[1], H.Sasaki[4], I.Yamamoto[6], T.Yanagita[7] and S.Vernetto[1]

1) Istituto di Fisica Generale, Universita di Torino, Torino, Italy
Istitute di Cosmogeofisica del CNR, Torino, Italy
2) National Institute of Polar Research, Itabashi, Tokyo, Japan
3) Institute for Cosmic Ray Research, University of Tokyo,Tokyo, Japan
4) Department of Physics, Kochi University, Koch, Japan
5) Department of Physics, Kobe University, Kobe, Japan
6) Faculty of Engineering, Okayama Univ. of Science, Okayama, Japan
7) Gunma college of Technology, Gunma, Japan

In order to detect primordial antimatter ($Z \geq 2$), a round Antarctic balloon flights is planned as Japan-Italy cooperative works. A new instrument consists of counter systems and a scintillation fiber tracking system. The scintillation fiber system will identify the antimatter among 10^{3-4} events which were selected with the counter system from the 10^{8-9} backgrounds. The Antarctic balloon experiment will reach flux sensitivities at 10^{-8} for antiprotons, 10^{-7} for antihelium and 10^{-6} for heavier antinuclei.

1. Introduction

There have been many search for antiprotons in cosmic rays[1]. However it is not easy to eliminate the antiprotons being produced by collisions of cosmic rays with interstellar matter from the observed antiprotons, because of uncertainties of production cross section and propagation model of cosmic rays. In order to study "primordial" antimatter (baryon symmetry/asymmetry study), we have to detect antinuclei with $Z \geq 2$, because the production probability of antinuclei from collisions of cosmic rays is very small.

The ratio of the extragalactic cosmic rays to the local cosmic ray fluxes is considered[2] as 10^{-5} to 10^{-4}. If the universe were baryon symmetric[3], about a half of extragalactic cosmic rays would be antimatter. The flux of antimatter will be reduced by fragmentation processes. Our cluster of galaxies might be made of matter. Then an experiment with at least a flux sensitivity of the 10^{-7} level is required to study "primordial" antimatter. However, the best limit remains around 10^{-4} for antinucleus[4]. The Antarctic balloon experiment will reach flux sensitivities at 10^{-7} level for antiheliums, and 10^{-6} level for heavier antinuclei.

SEPARATION OF SYNCHROTRON AND THERMAL EMISSION IN SPIRAL GALAXIES

Nebojsa Duric and David S. Dixon
Institute for Astrophysics
Department of Physics and Astronomy
University of New Mexico
Albuquerque, NM 87131
U.S.A.

Abstract

High resolution radio continuum images of galaxies contain information on synchrotron emitting regions where cosmic ray electrons are present. At higher radio frequencies thermal bremsstrahlung emission can also be present. Thermal emission traces regions of recently formed stars. The star forming regions are sites of type II SN and their remnants, a popular candidate for cosmic ray production. This paper describes a technique that combines multi-frequency radio images to produce separate maps of synchrotron and thermal emission for the purpose of comparing distributions of cosmic ray electrons and their possible sources.

Introduction The integrated emission of spiral galaxies is dominated by the synchrotron mechanism at frequencies below 5 GHz. This emission is believed to originate from cosmic ray electrons radiating in interstellar magnetic fields. Synchrotron emission maps can therefore be used to infer the distributions of cosmic ray electrons in the disks of other galaxies. However, for spatially resolved galaxies thermal bremsstrahlung (free-free radiation) can be an important contributor of emission in localized regions. Thermal emission arises from the free-free interactions of ions and electrons in HII regions, regions of ionized gas surrounding hot, recently formed stars. The thermal emission therefore provides a mechanism for tracing star forming regions. When both emission mechanisms are present it is difficult to interpret the radio emission properly. A method for separating the two forms of emission is therefore clearly desirable (Duric, Bourneuf and Gregory, 1988). In this paper we describe a technique for decomposing the radio emission into its two components. The separation technique has been coded into a algorithm that runs under the Astronomical Image Processing System (AIPS) and is described in more detail in the next section.

Technique Assuming that the emission from the region represented by image pixel (i,j) is a linear combination of a thermal component, a synchrotron component, and a small error:

$$S_{ij} = A_{ij}\nu^{-1} + B_{ij}\nu^{-\alpha_{ij}} + \epsilon_{ij}$$

where

S_{ij} is the total flux at pixel (i,j), A_{ij} is the thermal coefficient, B_{ij} is the synchrotron coefficient, α_{ij} is the spectral index at pixel (i,j), ν is the frequency and ϵ_{ij} is the error at pixel (i,j).

The program requires input images for at least three frequencies to return linear estimates of the coefficients, four frequencies for an error estimate. The fitting procedure is as follows:

1. Reject pixels for which one or more of the input maps is below a minimum number of standard deviations above zero.

2. Estimate the spectral index from the two longest wavelength maps.

3. Calculate the synchrotron coefficient using the estimated spectral index and assuming that all the emission at the longest wavelength is synchrotron.

4. Use the spectral index and synchrotron coefficient to calculate the synchrotron contribution at the shortest wavelength. Calculate the thermal coefficient from the difference between the shortest wavelength map and the synchrotron estimate.

5. Iterate the fitting routine until either

a) The χ^2 error estimate is less than or equal to the number of degrees of freedom (the number of input maps minus three), or

b) A maximum number of iterations is exceeded.

Initial Estimate An initial estimate of the coefficients and the spectral index can be made from as few as three maps. Fundamental to the estimation is the assumption that the synchrotron mechanism dominates at low frequencies. If the frequencies of the maps are ordered low to high such that S_1 represents the map at the lowest frequency ν_1, and S_N represents the map at the highest frequency ν_N, the assumption is that

$S_1 \approx B\nu_1^{-\alpha}$ and $S_2 \approx B\nu_2^{-\alpha}$ so that $\alpha_0 = \ln(S_1/S_2)/\ln(\nu_2/\nu_1)$ and $B_0 = S_1\nu_1^{-\alpha_0}$.

If α is much greater than 0.1 then the thermal component will be more evident at the highest frequency than at the lowest frequency. With this assumption, if $B_0\nu^{-\alpha_0}$ is extrapolated to the highest frequency, the result will be slightly less than S_N, the difference being attributable to the thermal component $A\nu^{-1}$. That is

$$A_0\nu_N^{-1} = S_N - B_0\nu_N^{-\alpha_0}$$

so

$$A_0 = S_N\nu_N^1 - B_0\nu_N - \alpha_0^1$$

The approximations for α_0, A_0, and B_0 are accurate within a few percent when the thermal component contributes less than ten percent of the total flux. For larger thermal fractions some number of iterations of the fitting procedure is

mandatory. Furthermore, an α_0 very near 0.1 results in a degeneracy, making A and B indistinguishable. In this case it is assumed that the emission is entirely thermal and that no further fitting is necessary.

Fitting Routine At present the downhill simplex method(Press et al, 1986), though generally slow to converge, is the most robust. The simplex method begins with an object defined by N+1 points in N-parameter space. In this case, four points in the space defined by the two coefficients and the spectral index. The trial function is evaluated at each of the N+1 points. Adjustments are made to the point at which the trial function differs the greatest from the data point. The adjustment will either shrink, stretch, or reflect that point through the other N points. The adjustment which results in the smallest volume which contains the data point is retained. The adjustment process is repeated for whichever trial point is now furthest from the data point.

The first initial point is the initial estimate described above. Assuming that α_0 is underestimated slightly, the second point is the first point moved out along the α-axis by ten percent. If α_0 is underestimated, then so is B_0, so point three is the initial point moved out along the B-axis by ten percent. Finally, the previous assumptions mean that the extrapolation of $B_0\nu^{-\alpha_0}$ is too low and that A_0 is overestimated, so the fourth point is the initial point moved in along the A-axis by ten percent. Ideally the simplex described by these four points contains the solution and it's now a matter of iterating until convergence.

Results We have chosen the spiral galaxy NGC4736 as the prototype for this study. The original observations made at 4 different radio continuum frequencies are shown in figures 1a, 1b, 1c and 1d. After processing with the routine, maps of synchrotron and thermal emission were generated. The thermal map is shown in figure 1e. As a check on the method, we compared the thermal map with an optical Hα image (figure 1f). Hα emission arises from the same HII regions producing the thermal radio emission. It is clear that the Hα image has a similar morphology to the thermal radio map. There are some minor discrepancies between the two maps but these can, for the most part, be explained by the fact that the Hα emission is subject to extinction by dust while the thermal radio emission is not. In future work, a quantitative assessment of the program's performance will be made. At present, the qualitative agreement with independent data suggests that the technique described here will be useful in astrophysical studies of CR distributions in other galaxies.

References

Duric,N.,Bourneuf,E., and Gregory,P.C. (1988) Astron. J. **96**, 1.

Press,W.H., Flannery,B.P., Teukolsky,S.A., Vetterling,W.T. (1986), *Numerical Recipes* (Cambridge University Press, Cambridge), p.289.

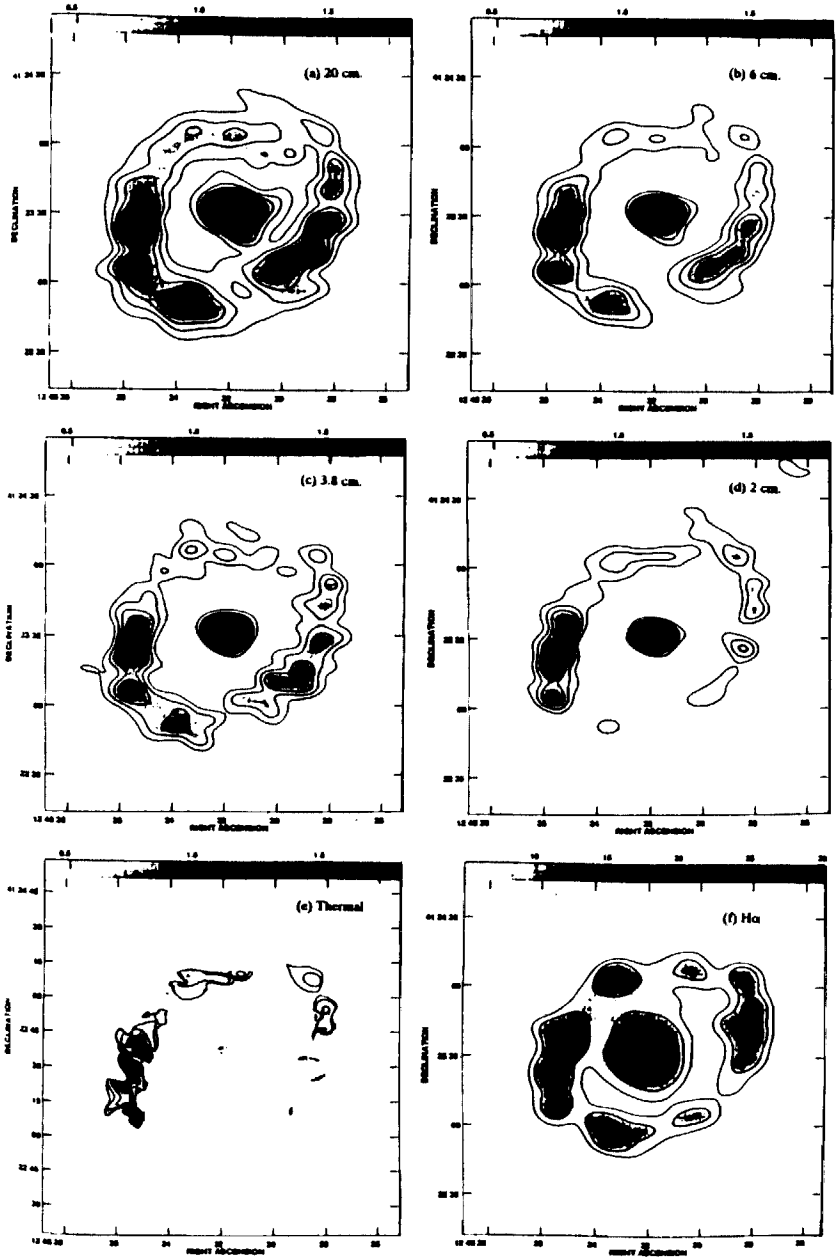

Figure (1) NGC4736. Flux contours for (a) through (e) at 0.4, 0.6, 0.8, 1.0, 1.2, 1.4, 1.6, 1.8, 2.0 millijanskys. The scale for (f) is arbitrary.